Conference on Modelling Fluid Flow (CMFF'22)
The 18th International Conference on Fluid Flow Technologies
Budapest, Hungary, August 30 -September 2, 2022

EFFECTS OF VALVE CHARACTERISTICS AND FLUID FORCE ON VALVE STABILITY

Gergely KESZTHELYI[1], Jürgen SCHMIDT[2], Jens DENECKE[3]

[1] Corresponding Author. CSE Center of Safety Excellence gGmbH. Joseph-von-Fraunhofer-Str. 9, D-76327 Pfinztal, Germany. Tel.: +49 721 6699 4837, E-mail: gergely.keszthelyi@cse-institut.de
[2] CSE Center of Safety Excellence gGmbH., e-mail: juergen.schmidt@cse-institut.de
[3] Hochschule Karlsruhe; CSE Center of Safety Excellence gGmbH. e-mail: jens.denecke@cse-institut.de

ABSTRACT

More than 10 models are available in the literature to protect emergency relief lines against valve instabilities and are proposed for the replacement of the 3% rule. They differ in assumptions and simplifications. Literature models to evaluate the stability of spring-loaded safety valves in gas service that can be used to predict an allowable inlet line length are classified, and a representative example of them is introduced more deeply to the readers.

The change in the fluid force acting on the disk is introduced, and two methods of modelling are shown, including measurement results from both literature and from the authors. The effect of the changing of the fluid force during the opening is described in relation to the models investigated, and it is shown that not all models are capable of taking the changes in the fluid force into account.

Two models are expanded to consider the effects of the changing fluid force during the opening of the valve and are compared to simulation results, which show that the expanded models are capable of predicting the effect of the change, unlike their original forms.

Keywords: chatter, fluid force, safety valve, valve instability

NOMENCLATURE

API American Petroleum Institute

A_{eff}	$[m^2]$	effective area
$\hat{A}_{eff}$	$[m^2]$	normalised effective area
F	$[N]$	force
L	$[m]$	inlet line length
a	$[m/s]$	speed of sound
c	$[Ns/m]$	damping
k	$[N/m]$	spring stiffness
m	$[kg]$	moving mass
$\dot{m}$	$[kg/s]$	mass flow
t	$[s]$	time
t_{open}	$[s]$	opening time
w	$[m/s]$	fluid velocity
x	[m]	current position of the disk
x_0	[m]	spring pre-compression
ρ	$[kg/m]$	density
θ	[°]	discharge angle
ω_n	[rad/s]	natural frequency

Subscripts and Superscripts

close	closed the safety valve
f	fluid
face	disk face
open	fully open safety valve
n	nozzle

1. INTRODUCTION

Safety valves serve the purpose of protecting against overpressure, and as such their stable operation is necessary for the safety of the protected system. Experimental evidence has shown that stable operation is not guaranteed in all conditions, and instability can appear in the forms of chatter and flatter [1].

One of the sources of these instabilities is the piping connected to the safety valve, especially the inlet line leading up to it. Models to avoid chatter caused by the inlet line have been researched since Sylvander and Katz's [2] initial research for the API in 1948. Their research has evolved into the three percent rule, which is currently in both the API 520 Part II [3] and ISO4126-9 [4] standards. This rule in its current form limits the non-recoverable pressure loss in the inlet line to three percent of the set pressure of the safety valve. It is based on steady state flow through the valve and was not originally intended to avoid dynamic instabilities.

Research into other methods of determining stability has been ongoing since the adoption of the three-percent rule, with Darby [5] finding more than 50 publications regarding the stability of the safety valve. Even as many of these do not contain new stability models, or contain models that have been later on improved by their authors, the CSE Institute [6] has identified more than 10 stability models.

In this paper the scope of investigation is limited to models capable to size safety valves for gas service and that do not solve the whole transient movement of the safety valve. The latter means that there will be no Computational Fluid Dynamics (CFD) models reviewed, as they are typically too time consuming for industrial purposes.

2. MODEL DESCRIPTION AND COMPARISON

Models can be categorised based on the assumed source of the instability. Reviewing models from the last 30 years, four main categories of models have been identified:

Balance-based models are based on a pressure balance on the valve disk, consisting of the losses in the inlet line, the set pressure and the reseating pressure. The models of Singh [7] and Melhem's simple force balance [8] are examples of this category, along with of course the three-percent rule itself.

The *pressure wave* models limit the size of the initial waves in the system, based on either the reseating pressure or the set pressure. This category includes the pressure surge model of Frommann and Friedel [9], later improved by Cremers et al. [10].

Stability analysis models operate based on the assumption that a working point exists. A stability analysis in the complex frequency domain is then conducted to determine if the working point is stable. Such models have been previously created by MacLeod [11] and Kastor [12] back in the 80ies, and more recently by Izuchi [13].

The quarter wave model of Hős [14] models the pressure distribution according to the first harmonic of the system, and evaluates the system based on that.

All the models listed above except for the MacLeod model (which is for systems without an inlet line) share the assumption or have such a result, that safe operation of a safety valve can be secured by proscribing a maximum permissible inlet line length.

The various models within a category are rather similar, and as such only the most precise representative will be chosen from them. As such this paper will limit its scope the to the Melhem's [8] *simple force balance* method, the *improved surge model* by Cremers [10], the *Izuchi* model [13] and the *quarter-wave model* of Hős [14].

2.1 Basic equations of the system

The movement within the valve is modelled by all models as a simple spring-mass-damper system moved by the fluid force:

$$F_f = m \cdot \ddot{x} + c \cdot \dot{x} + k \cdot (x + x_0) \tag{1}$$

with x_0 being the length of spring pre-compression necessary for the valve to open at the given set pressure, and as such can be calculated from it. On the right side of the equation, the moving mass m and the spring stiffness k, while not directly available in the manufacturer's catalogues, can be measured directly, without mounting the safety valve on a test rig. The fluid force F_f and the damping c however are affected by many hard to measurable, or changing variables during even the installation, for example the damping containing the friction forces acting upon the disk or the spindle.

Another assumption shared between models is the size of the initial pressure wave in the system. E.g., in the pressure wave models, and some balance-based models, it is calculated as a Joukowsky shock wave, and its maximum value is:

$$\Delta p_{max} = \rho \cdot a \cdot w \tag{2}$$

with the ρ being the density in the upstream vessel, and a the speed of sound in the same location. w is the velocity of the fluid in the pipeline system, which is calculated from the mass flux flowing through the fully open safety valve.

The wave pressure considered to linearly increase with time, starting on the set pressure, up until reaching the return time of a wave in the inlet line. The return time is calculated as twice of the length of the inlet line L divided by the stagnation speed of sound in the upstream vessel. This means that at the time of the valve has fully opened, the wave pressure above the set pressure is:

$$\Delta p(t_{open}) = \Delta p_{max} \cdot \frac{t_{open}}{\frac{2 \cdot L}{a}} \tag{3}$$

The opening time is usually not provided by the manufacturer and can only be measured if the safety valve is connected to a system. To avoid this, various empirical correlations exist for the determination of the opening time [8].

2.2 Description of models

The *improved surge* model is based on limiting the initial Joukowsky wave of the opening to the difference between the set pressure and the blowdown. This is done by rearranging the terms found in Eqs. (2) and (3) to solve for the initial inlet line length. The model also provides an empirical method of calculating the opening time, which as mentioned previously is not available in manufacturer catalogues.

The *simple force balance* method is based on calculating the pressures acting on the safety valve disk and comparing them to the blowdown pressure. Reaching the blowdown pressure, the valve is assumed to close. The included pressures are the set pressure, the back pressure, the pressure loss in the inlet line due to friction, and the wave pressure traveling through the inlet line with the speed of sound. As such, it includes more variables than the *improved surge* model, but as the wave pressure is significantly larger than the pressure loss, it is the more important factor in the stability, leading to both models dependent just on the initial wave, i.e., neglecting the frictional losses.

The *Izuchi* model is based upon on the wave equation for the pressure change in the inlet line, while neglecting the effects of the friction in the inlet line, and assuming the system is undamped. Based on this equation, combined with the spring-mass-damper equation seen in Eq. (1), a transfer function is created for the movement of internals in the safety valve. This transfer function is then used for a traditional stability analysis. The final formulation of the Izuchi equation published in [13] is:

$$L = \frac{\pi a}{2\omega_n \sqrt{\frac{x + x_0}{x}}} \quad (4)$$

where ω_n is the natural frequency of the safety valve, calculated as the square root of the spring stiffness divided by the mass considered to be moving. The lift of the safety valve is an input leading to an increasing maximum length with increasing lift. The lift is either calculated by assuming that the safety valve is stable, with the fluid force in Eq. (1) being in balance with the spring forces, or a full lift is assumed.

The *quarter wave model* has formulations of various complexity. Taking one that does not take into account the friction loss in the inlet line, and also assumes the system has no damping (which are assumptions shared with Izuchi), the following closed form equation can be derived:

$$L = \frac{\pi a}{2\omega_n \sqrt{2 \cdot \frac{x + x_0}{x} + 1}} \quad (5)$$

Note that even though the initial idea is different, the final forms of the equations are similar, only differing in constants in the divisor. This means that of these two models the *quarter wave* model will always predict a shorter allowable inlet line length.

3. CHANGES IN THE FLUID FORCE

The fluid force acting on the valve disk is changing during the opening of the safety valve and is the source of the pop opening of the safety valve. This variable is however otherwise not explicitly included in the models listed previously.

This means that the fluid force of Eq. (1) is not a constant force but varies during the opening of the safety valve. The change in fluid force is experimentally proven to be dependent on the valve type (e.g., disk geometry), the valve lift and as a minor effect on the pressure in the vessel and fluid properties. Physically, it is expected to be affected by the spindle friction, flow separation below the valve disk, fluid contraction and redirection within the valve, deflection angle of the fluid at the valve disk, turbulence and vortex creation in the valve housing and several other parameters.

Simplifying the effects on the fluid force, two main models of describing the change in force exist, the *discharge angle* and the *effective area*.

In the discharge angle model, the changes due to flow separation, contraction and redirection are modelled by an average angle representing the fluid force acting on the lower side of the disk. Such definitions of force were used by Singh [7], and most recently Darby [5], though with slightly different formulations. Using the formulation of Darby, the equation for the fluid force is described as:

$$F_f = (p_{in} - p_{back}) \cdot A_n + \\ + \dot{m}^2 \left(\frac{sin(\Theta)}{\rho\pi(x - x_0)} + \frac{1}{\rho \cdot A_{face}} \right) \quad (6)$$

where Θ is the angle between the horizontal and the direction of the fluid, A_n is cross sectional area of the nozzle, and A_{face} the area is the downward facing side of the valve disk,

To increase the precision of the model, a linear change in the discharge angle with valve lift is assumed, where the current angle can be calculated as a linear interpolation between the angles when the valve is closed and is fully open

$$\Theta(x) = \Theta_{closed} + \frac{x}{x_{max}} \cdot (\Theta_{open} - \Theta_{\mathrm{closed}}) \quad (7)$$

With this linear correlation for the angle the correlation between the force and the lift is a part of a sinusoidal curve.

Another option is to define the force simply as the pressure difference between the pressures at the inlet and the outlet of the safety valve acting on a theoretical, so-called effective area. In this case the fluid force is defined as:

$$F_f = A_{eff}(x) \cdot (p_{in} - p_{out}) \quad (8)$$

with the effective area usually only considered dependent on the current position of the valve disk. To simplify comparisons, the effective area is often converted to a dimensionless variable by dividing it by the flow area of the nozzle:

$$\hat{A}_{eff}(x) = \frac{A_{eff}(x)}{A_n} \quad (9)$$

Herewith, relative effective areas are independent of the size of the safety valve.

The effective area contains all parameters not covered by the 1D ideal spring-mass system equation, as described above. Both the pressures, and the force acting on the disk can be directly measured, and hence the effective area may be deduced from experiments – at least under steady conditions. Generally, this are global measurements where the parameter affecting the relative effective area covered only implicitly.

An advantage of the model is that to calculate the lift of the stable solution, a single-variate ordinary equation can be written for the lift, by combining Eq. (1) in steady state with Eq. (8).

The relative effective area curve always starts at one as it is assumed that when the valve is closed, the forces directly act on the closed disk. To ensure a pop open, all other values of an effective area curve are taken larger than unity.

3.1. Measurements of the changing fluid force

An average discharge angle of the fluid below the valve disk is not provided by the manufacturers of safety valves. In the literature, such values were determined in dynamic experiments by Darby [15]. In his measurements, the Θ_{close} and Θ_{open} angles were obtained by fitting the measurement results to the equations, and assuming a linear change in discharge angle seen in Eq. (3).

As it can be seen in a visualisation of Darby's published measurement data [16] in Figure 1, the results are not conclusive, with the opening and closing angles being dependent not only on the set pressure, but also e.g. on the inlet line length.

This shows that the discharge angle varies with multiple parameters and is difficult for define for every specific valve size and type. Predictions, without a fit to measured values are not feasible.

The effective area is not included in the catalogues provided by the manufacturers, and there are few examples ([12],[13], [14]) in literature of it being depicted from experiments or simulated.

The earliest experimental determination of the effective area conducted by Kastor. A linear equation for the effective area was provided by the author in the appendix, along with the raw measurement data. Visualising the results, there is no real correlation, and the best linear fit had an $R^2 = 0{,}072$ error. This resulted in the author not using the linear fit due to its low accuracy, and instead opted for a constant value in their calculations.

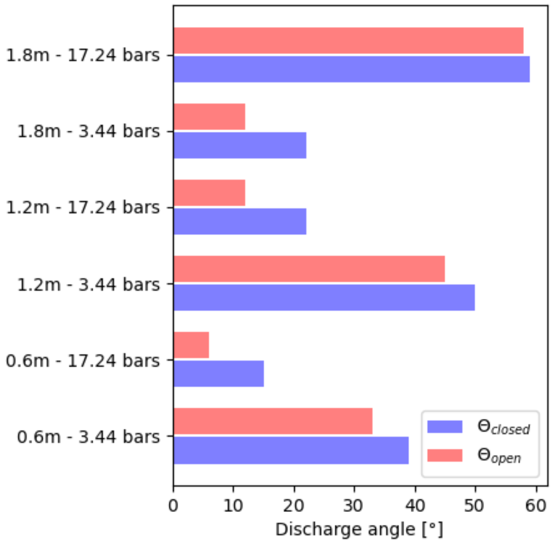

Figure 1. Discharge angles measured by Darby [16]

Izuchi [17] conducted his measurements with a removed spring, and a force measurement to determine the force acting on the disk, at fixed heights. The measurements were repeated with different fittings at the outlet of the safety valve, finding that the curve was highly dependent on the outlet size, with the effective area going below a value of one in case of large reducers.

Similar measurements [18] have also been conducted by the authors the at the CSE Test Loop on a DN25x40 European safety valve, using air as test fluid. In this these measurements, two set pressures (2 bar(g) and 10 bar(g)) and various backpressures, up to 60% of the set pressure were tested, going even beyond the back pressure allowed by the manufacturer.

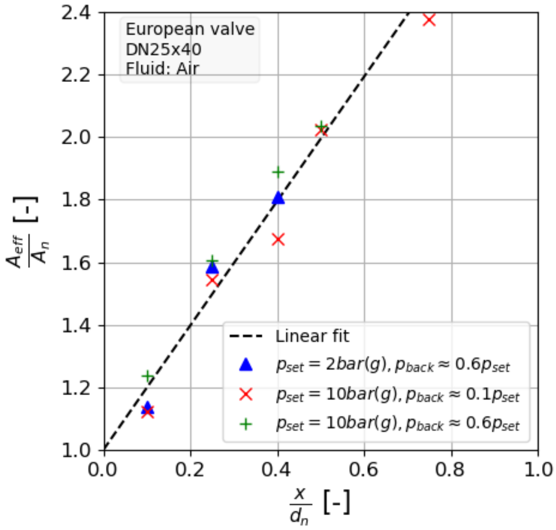

Figure 2. Effective area values measured at the CSE with different set and back pressures

The measurements were conducted with a steady flow, and a fixed lift of the valve disk, with the spring being removed, and replaced by a force sensor. It should be noted that during these kinds of measurements, the setup makes it impossible to measure the average fluid force at full lift, including the force acting on top of the disk in the valve housing.

In the measurements it was found that the effective area curve of the system developed from measurements was independent of both the back pressure of the system, and the set pressure, as the relative errors compared to the fitted curve lay below 16%, and the average error was below 10%. Some representative measurement data, along with the linear fit of the results can be seen in Figure 2.

The measurement results also line up with simple static, two-dimensional CFD simulations [19] conducted on the same valve geometry. Example results for simulations with different back pressures at 10 bar(g) set pressure can be seen in Figure 3, along with a second order fit. These simulations show good correlation with the measured results and were not dependent on the pressures the simulations conducted at. This is in line with the findings of Hős, who also had low variance in the effective area curves in his simulations.

None of the measurements or simulations of the effective area were conducted with a moving disk. This means that the measured values are possibly only approximations compared to a moving valve, as it could also be affected by other parameters, such as the speed of the disk. Further measurements need to be conducted to determine if the measurements with a fixed lift and a load cell are representative of the fluid force.

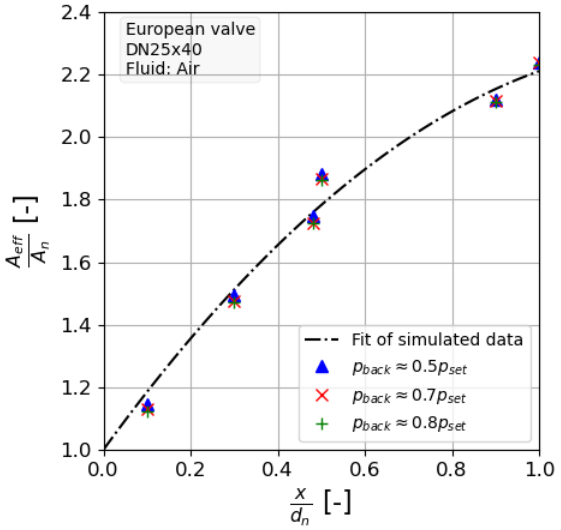

Figure 3. Results of two-dimensional CFD simulations with 10 bar(g) set pressure compared to the curve fitted on measurement values

As the effective area is more easily reproducible by measurements, and it has been used by authors whose models are being compared, it will be used further on as the model for the changing force of the fluid.

3.2. Effects of the changing fluid force on stability models

The change in fluid force depends mainly on two contradicting parameters - the enlargement of the area where the pressure acts on while opening the valve, and the decrease of the pressure below and the increase above the valve disk. At the beginning of the valve opening, the pressure decrease is dominating, hence, the fluid force typically decreases. With further increasing lift, the area increase becomes dominate and lead to larger fluid forces with lift. Typically, a fluid force curve is a 90° turned "s"-shaped to allow for an initially stable, proportional opening of the valve, where mainly spring and fluid forces are in equilibrium. Further opening to the so-called pop-point of the valve would lead to a tremendous excess force compared to the spring and a non-equilibrium of the forces pushing the valve disk to open. The acceleration of the moving masses in the valve heavily depends on the amount of excess force above the pop-point. The disk typically moves up either to a lift where forces become equal or to a geometrical lift limit, where the valve stays open. In case of a stable open of a safety valve, that is not at full lift, these fluid forces are in equilibrium with the spring force acting on the valve disk. Therefore, to properly predict the lift of a safety valve, it is important to know the forces acting on the valve disk.

In case the fluid force is calculated by the effective area model in a safety valve model, the relative effective area used must have values above one to explain the phenomena described in the previous paragraph. Calculating the opening with an effective area that is smaller than in reality would result in a partial opening of the safety valve.

The lift is a direct input for the *Izuchi* and *quarter wave models*, and as such the change of fluid force needs to be taken into account to determine this input parameter. An input of a smaller lift with these models predicts a shorter inlet line, meaning that using the maximum lift would not be conservative.

During the derivation of both models, the effective area was included during the initial phase of the derivations but was later simplified out. This means that both models can be revisited to include the relative effective area curves not just in the lift, but also as an input in itself. The Izuchi formulation in this case takes the form of:

$$L = \frac{\pi a}{2\omega_n \sqrt{\frac{x + x_0}{x} + 1 - \frac{\partial \hat{A}_{eff}(x)}{\partial x} \cdot x}} \quad (10)$$

The original paper [13] does not explain the reason for not including the additional term compared to Eq. (4). According to both personal correspondence with Izuchi, and the white paper of Melhem [20], the reason for the simplification was that the effective area curves were of a shape that the $\frac{\partial \hat{A}_{eff}}{\partial x} \cdot x$ part was close to unity at the full lift of the valve, allowing for a simplification of the equation.

During the derivation of the final formula of the quarter wave model shown in Eq. (5), the relative effective area was assumed to be equal to one, simplifying the calculations, which would not explain a real pop open of a valve. In case of continuing the derivation without this simplification, one arrives at the solution:

$$L = \frac{\pi a}{2\omega_n \sqrt{2 \cdot \frac{x + x_0}{x} \cdot \hat{A}_{eff} + 1}} \qquad (11)$$

Note that the two calculation methods, even though they used the same inputs in their simpler forms, they use the effective area curves differently, with the *Izuchi* model using the derivative, and the *quarter wave* using the actual value.

To investigate the theoretical effects of the effective area on the calculated stability of safety valves, one-dimensional CFD simulations with various constant $\hat{A}_{eff}$ values ranging from 1.0 to 2.0 were carried out. The CFD simulations represent an precise solution of an ideal system without the simplifications made in the different models and may be taken to evaluate the assumptions and simplifications implicitly given in the models and also in the expended models seen in equations (10) and (11).

The CFD simulations were based on ideal gas with friction, using a Lax-Wendroff solver in the inlet line. The safety valve was modelled by solving Eq. (1) with a variable step Runge-Kutta method, and the fluid force was calculated using the effective area as described in Eq. (8). Choking was assumed in the smallest cross section in the safety valve to calculate the mass flow leaving the system. The vessel pressure was kept constant during the simulations. Inlet line friction was neglected.

The tested valve was a DN50x80 valve from a European manufacturer, with a nozzle diameter of 46 mm, and a maximum lift of 15.5 mm. This valve had been previously measured at the CSE Institute, and had allowable measurement length results for comparison [21], having started to chatter with an inlet line length of one meter. The released fluid was air at 5.8 bar(g) and 300 K.

The CFD simulations were run in 5-centimetre steps between 0.4 and 1.4 meters of inlet line length. As some simulations might be stable, even if a simulation with a lower line length was unstable, all simulation results are plotted, with the stable and unstable simulations being marked separately, a red plus, and a green x respectively.

The simulation results are compared against the compared to the expanded *Izuchi* and *quarter wave models* described in Eqs.(10) and (11). The lift as an input for these cases was calculated with the vessel pressure to keep with the assumption of the models regarding the lack of friction in the inlet line.

The results of the comparison can be seen in Figure 4. The simulations show that in case of a relative effective area of 1.6 and 1.8, there is an area of instability, but higher inlet line lengths were simulated as stable. Full lift was reached with a relative effective area of 1.8. This influenced the inlet line lengths calculated from the expanded *Izuchi* and *quarter wave models*. It is also the reason for the increase in the permissible inlet line in case of effective areas below 1.8, following the simulated trend.

After the full lift was reached, the predicted inlet line length of *quarter wave model* was decreasing as the effective area appears in the divisor for this model. This highlights, that even after reaching full lift, the chosen effective area model does have an effect on the allowable inlet line length predicted by the model.

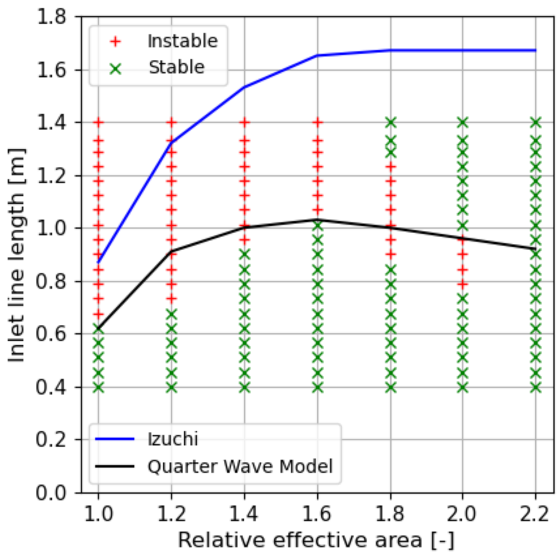

Figure 4. The allowable inlet lines according to the Izuchi and QWM models compared to one-dimensional simulations, with a constant effective area

To test the effect of different effective area curves, simulations and calculations with a constant effective area slope were also conducted, with the relative effective area curve taking the form:

$$\hat{A}_{eff}(x) = 1.0 + slope \cdot \frac{x}{x_{max}} \qquad (12)$$

The slopes tested ranged from 0, to 1.0, meaning that the maximum dimensionless effective areas ranged between 1.0 and 2.2, covering the same range as the constant effective areas in the simulations shown in Fig. 4. The maximum lift was reached with a slope of 0.8, after which the lift for the models was taken as the maximum available lift. The results of the simulations and the extended Izuchi and quarter wave models with an effective area changing linearly can be seen in Figure 5.

Noticeably, in this case, there are no simulations that predicted stable valve movement when a simulation with a smaller inlet line length predicted instability. The trends are similar as with the constant inlet line lengths, with larger effective areas meaning a stabler opening.

Note that in this case, both models predicted a lower allowable inlet line length as the maximum opening was reached. As the derivative of the effective area curve being calculated was positive, not only the *quarter wave* but also the *Izuchi* model decreased by higher effective areas, which appeared after full lift was reached.

The *simple force balance, pressure surge models* and the *three percent rule* were not compared to the simulations. These models evaluate the stability based on empirical relations at the nominal lift given by the manufacturer or are experimentally evidenced conventions like the three precent rule. A true lift based on the force balance on the valve disk is not considered.

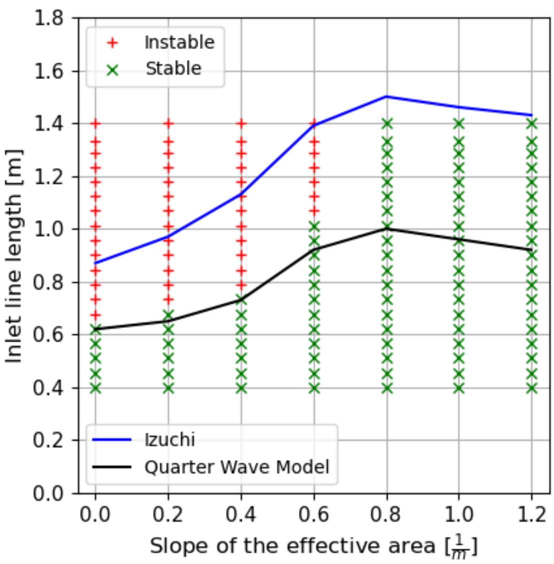

Figure 5. The allowable inlet lines according to the Izuchi and QWM models compared to one-dimensional simulations, with a linearly changing effective area

The results show that in general, a larger effective area increased the stability of the calculated system in the case of both the constant and the linearly changing effective area. This was the case even if full lift was reached, as the effective area or its derivative appear in the *quarter wave* and the *Izuchi* models respectively.

Looking at Figs. 4 and 5 in both cases the minimum length is reached at a constant relative effective area of one. In this case, the expanded *Izuchi* model would take a form similar to the one published in [13], but have an additional term of plus one under the square root in the divisor, predicting a lower inlet line length than the currently published model. In the case of a constant effective area of one, the *quarter wave* model would be unchanged, resulting in only one constant multiplicator difference for the two models.

Note however, that a relative effective area of constant one does not guarantee that the minimum predicted allowable inlet line length of the models will be minimal, that is also dependent on other parameters of the system such as the maximum lift, the set pressure and the spring stiffness. These results show that the effective area is a parameter that needs to be taken into account before calculating using these methods.

4. CONCLUSIONS

Four different categories of models have been introduced, with the classification based on the initial assumptions of the authors of models. A representative example of all four models has been sought out, and their working methods compared, highlighting the differences in their approaches.

The change in fluid force during the opening was introduced and shown to be a necessary component of the operation of pop open safety valves. Only three independent effective area measurements were found in literature however, and as such the parameter is deemed to be under investigated, and its dependencies on factors other than the lift have not been fully examined.

The ways it can affect the various stability models has been shown. The results showed that the *simple force balance*, *improved pressure surge* and the *three-percent rule* are all unaffected in their current formulations, as in the models a full lift is assumed during the calculation of the stability criterion.

The Izuchi and quarter wave however use the lift of the safety valve as an input parameter. Therefore, these models were expanded from their derivations to include the effective area, and using these forms, the effect of the effective area on their predictions were calculated and were compared to one-dimensional CFD simulations. The expansion of the *Izuchi* and *quarter wave models* managed to follow the trends that were simulated. These simulations have also shown that the effective area influences the calculated stability of the safety valve,

As such it can be determined that the changes in fluid force cannot be neglected and needs to be taken into account for the predictions to be precise. Further measurements are needed to determine if the effective area is dependent upon other parameters as well, or only the lift as it is currently assumed.

REFERENCES

[1] American Petroleum Institute (API), *Sizing , Selection , and Installation of Pressure-Relieving Devices in Refineries Part I — Sizing and Selection*, 6th ed., vol. 1, no. July 2014. 2014.

[2] N. E. Sylvander and D. L. Katz, “The Design and Construction of Pressure Relieving Systems,” Ann Arbor, 1948. doi: 10.1038/087240a0.

[3] American Petroleum Institute (API), *Sizing, Selection, and Installation of Pressure-relieving Devices; Part II—Installation*, 6th ed., no. March. 2015.

[4] International Organization for Standardization, “ISO 4126-9 Safety devices for protection against excessive pressure - Application and installation of safety devices excluding stand-alone bursting disc safety devices,” vol. 2008. 2008.

[5] R. Darby, “The dynamic response of pressure relief valves in vapor or gas service, part I: Mathematical model,” *J. Loss Prev. Process Ind.*, vol. 26, no. 6, pp. 1262–1268, Nov. 2013, doi: 10.1016/j.jlp.2013.07.004.

[6] G. Keszthelyi, J. Schmidt, and J. Denecke, “Evaluation and comparison of safety valve chatter prediction models.” *DIERS Spring meeting* 2021.

[7] A. Singh, “On the Stability of a Coupled Safety Valve-Piping system,” in *Testing and Analysis of Safety / Relief Valve Performance*, 1982, pp. 29–37.

[8] G. A. Melhem, “Analysis of PRV Stability In Relief Systems Part II - Screening,” Salem, 2016.

[9] O. Frommann and L. Friedel, “Analysis of safety relief valve chatter induced by pressure waves in gas flow,” *J. Loss Prev. Process Ind.*, vol. 11, no. 4, pp. 279–290, Jul. 1998, doi: 10.1016/S0950-4230(97)00040-5.

[10] J. Cremers, L. Friedel, and B. Pallaks, “Validated sizing rule against chatter of relief valves during gas service,” *J. Loss Prev. Process Ind.*, vol. 14, no. 4, pp. 261–267, Jul. 2001, doi: 10.1016/S0950-4230(00)00054-1.

[11] G. MacLeod, “Safety Valve Dynamic Instability: An Analysis of Chatter,” *J. Press. Vessel Technol.*, vol. 107, no. 2, p. 172, 1985, doi: 10.1115/1.3264430.

[12] K. A. Kastor, “Chatter Instability of Spring Loaded Relief Valves,” University of Delaware, 1986.

[13] H. Izuchi, “Stability Analysis of Safety Valve,” *Proc. Dyn. Des. Conf.*, vol. 2008, no. 0, pp. 238-1-238–6, 2008, doi: 10.1299/jsmedmc.2008._238-1_.

[14] C. J. Hős, “Direkt rugóterhelésű biztonsági szelepek dinamikus viselkedése és stabilitása,” Budapest University of Technology and Economics, 2019.

[15] A. A. Aldeeb, R. Darby, and S. Arndt, “The dynamic response of pressure relief valves in vapor or gas service. Part II: Experimental investigation,” *J. Loss Prev. Process Ind.*, vol. 31, no. 1, pp. 127–132, Sep. 2014, doi: 10.1016/j.jlp.2014.06.002.

[16] R. Darby and A. A. Aldeeb, “The dynamic response of pressure relief valves in vapor or gas service. Part III: Model validation,” *J. Loss Prev. Process Ind.*, vol. 31, pp. 133–141, Sep. 2014, doi: 10.1016/j.jlp.2014.06.001.

[17] H. Izuchi, “Chatter Of Safety Valve,” *API 2008 Fall Meeting*. pp. 1–60, 2008.

[18] C. B. Dinh, “Modellentwicklung zur Untersuchung des Flatterns eines Sicherheitsventils,” Hochschule Karlsruhe, 2021.

[19] S. Kempf and S. Kinalicukur, “Experimente zu Hubbegrenzung und Gegendruck,” Hochschule Karlsruhe, 2020.

[20] G. A. Melhem, “PRV Stability Inlet Line Critical Length.” Salem, pp. 1–11, 2021.

[21] J. Schmidt and J. Denecke, “European Program on Investigation of Valve Instabilities (EuroValve) Part I: Experimental investigation,” *Joint US and European DIERS User Group Meeting* 2019.